Estimation of Land Surface Temperature from Landsat-8 OLI Thermal Infrared Satellite Data. A Comparative Analysis of Two Cities in Ghana

Yaw A. Twumasi[1*], Edmund C. Merem[2], John B. Namwamba[1], Olipa S. Mwakimi[3], Tomas Ayala-Silva[4], Diana B. Frimpong[1], Zhu H. Ning[1], Abena B. Asare-Ansah[1], Jacob B. Annan[1], Judith Oppong[1], Priscilla M. Loh[1], Faustina Owusu[1], Valentine Jeruto[1], Brilliant M. Petja[5], Ronald Okwemba[1], Joyce McClendon-Peralta[1], Caroline O. Akinrinwoye[1], Hermeshia J. Mosby[1]

[1]Department of Urban Forestry and Natural Resources, Southern University and A&M College, Baton Rouge, Louisiana, USA
[2]Department of Urban and Regional Planning, Jackson State University, Jackson, Mississippi, USA
[3]Institute of Resource Assessment, University of Dares Salam, Dares Salam, Tanzania
[4]USDA-ARS Tropical Agriculture Research Station, Mayaguez, Puerto Rico, USA
[5]Water Research Commission (WRC) Private Bag X03, Gezina, South Africa
Email: *yaw_twumasi@subr.edu, *yaw.twumasi@gmail.com

How to cite this paper: Twumasi, Y.A., Merem, E.C., Namwamba, J.B., Mwakimi, O.S., Ayala-Silva, T., Frimpong, D.B., Ning, Z.H., Asare-Ansah, A.B., Annan, J.B., Oppong, J., Loh, P.M., Owusu, F., Jeruto, V., Petja, B.M., Okwemba, R., McClendon-Peralta, J., Akinrinwoye, C.O. and Mosby, H.J. (2021) Estimation of Land Surface Temperature from Landsat-8 OLI Thermal Infrared Satellite Data. A Comparative Analysis of Two Cities in Ghana. *Advances in Remote Sensing*, **10**, 131-149.
https://doi.org/10.4236/ars.2021.104009

Received: June 13, 2021
Accepted: October 12, 2021
Published: October 15, 2021

Abstract

This study employs Landsat-8 Operational Land Imager (OLI) thermal infrared satellite data to compare land surface temperature of two cities in Ghana: Accra and Kumasi. These cities have human populations above 2 million and the corresponding anthropogenic impact on their environments significantly. Images were acquired with minimum cloud cover (<10%) from both dry and rainy seasons between December to August. Image preprocessing and rectification using ArcGIS 10.8 software were used. The shapefiles of Accra and Kumasi were used to extract from the full scenes to subset the study area. Thermal band data numbers were converted to Top of Atmospheric Spectral Radiance using radiance rescaling factors. To determine the density of green on a patch of land, normalized difference vegetation index (NDVI) was calculated by using red and near-infrared bands *i.e.* Band 4 and Band 5. Land surface emissivity (LSE) was also calculated to determine the efficiency of transmitting thermal energy across the surface into the atmosphere. Results of the study show variation of temperatures between different locations in two urban areas. The study found Accra to have experienced higher and lower dry season and wet season temperatures, respectively. The temperature ranges corresponding to the dry and wet seasons were found to be 21.0985˚C to 46.1314˚C, and, 18.3437˚C to 30.9693˚C respectively. Results of Kumasi also show a higher range of temperatures from 32.6986˚C to 19.1077˚C during the dry season. In the wet season, temperatures ranged from 26.4142˚C to

−0.898728˚C. Among the reasons for the cities of Accra and Kumasi recorded higher than corresponding rural areas' values can be attributed to the urban heat islands' phenomenon.

Keywords

Remote Sensing, Land Surface Temperature (LST), Atmospheric Spectral Radiance, Normalized Difference Vegetation Index (NDVI), Land Surface Emissivity (LSE), Landsat 8 Satellite, Ghana

1. Introduction

Land surface temperature (LST) plays an important role in the urban environment [1]. Hence, it must be considered in the analysis of urban thermal environment and behavior. Its environmental influence is also felt at regional and global levels. Xiao *et al.* [2] studied the influence of land-use and land-cover (LULC) on land surface temperature through combining remote sensing and geographic information system (GIS) techniques for the detection of the spatial variation of land surface temperature. They also used these techniques to determine the quantitative relationship of land surface temperature with some biophysical and demographic variables based on statistical modeling for Beijing' central area. The proportion of forest, water, and farmland per grid cell imagery was found to explain 71.3 percent of Beijing's LST variance [2]. According to this study, land surface temperature was found to be positively correlated with the percentage of low density built up, high density built-up, extremely high buildings, low buildings per grid cell, and population density. The study found negative correlations to exist between, land surface temperature with the percentage of forest, farmland, and water bodies per grid cell. The lower layer of the urban atmosphere's air temperature modulates the land surface temperature, which is also a primary factor in the determination of the radiation from the surface and energy exchange. It also influences human comfort and buildings' internal climates, in urban area buildings [3]. The color of buildings, traffic loads, the sky view factor, the physical properties of structures, street geometry, view factor of the sky and human activities are important determinants of land surface temperature [4].

Replacement of vegetation by asphalt and concrete for construction of roads, buildings, and other structures for accommodation of growing urban populations leads to the formation of urban heat islands [5]. Anthropogenic heat emission caused by human population distribution also influences urban heat island (UHI) intensity [6], a contributor to the urban's land surface temperatures. Feng *et al.* [7] derived land surface temperatures at Suzhou City, for spring and summer 1996, 2004, and 2016, by using seven Landsat images. The spatial factors influencing the land surface temperature patterns were also examined. The factors

included land coverage indices, the LST location and proximity factors. The land coverage indices were found to be the most dominant factors of LST [7].

Studies of urban land surface temperature have yielded advanced numerical and physical models, including energy balance models [8] [9], three-dimensional simulations [10], laboratory models [11], Gaussian models [12], and other numerical simulations. Researchers have developed physical models, including energy balance models [8] [9], Gaussian models [12], laboratory models [11], three-dimensional simulations [10], and other numerical simulations.

Land cover plays an important role in land surface temperature. The drivers land-use/land-cover change were categorized by [13] into four classes, namely, political, demographic, economic, and environmental forces. High population growth rate, a demographic factor, frequently results in over exploitation of natural resources. Population growth is considered by scholars as a major driver of land use change, especially in developing countries [14] [15] [16]. Accra's urban population has expanded fast, leading to rising demand for housing facilities and corresponding infrastructure [17]. The rapid increase in Ghana's urban population is reflected in the expansion of the Settlements land cover class. In 1975, the urban areas covered 1460 km^2. In 2000 and 2013, it grew to 2560 km^2 and 3830 km^2, respectively [18]. Since the mid-1980s, Ghana has rapidly been urbanized. The country's population more than doubled between 1984 and 2013, with an annual population growth of 4.4%. During this period, Ghana's urban population grew from less than 4 million to almost 14 million [19]. A significant population of Ghanaians are urban dwellers, with approximately half of the Ghanaian population living in urban centers as of 2010. The population is expected to rise to 70% by 2050 [20].

In a study on growth of human population and increase of temperature, with the increase in urbanization, number of motor vehicles and magnitude of green area in Erzurum city, Turkey, [21], established that, there were statistically significant relationships between the growth of population and the maximum temperature. The variation between the number of vehicles and minimum temperature was also found to be statistically significant [21]. Addae and Oppelt [22] carried out a post classification change detection on several Landsat images to map and analyze the land use/land cover change extent and rate in the greater Accra metropolitan area for the period 1991 to 2015. The results of this study revealed that there was an increase of approximately 27.7% in built-up areas over the study period. Forest areas had however, experienced significant drops, decreasing from 34% in 1991 to 6.5% in 2015. Land use map projections by [22] show that 70% of the study area in Accra, Ghana will be urbanized, a significant rise in comparison to 44% in 2015. This rise could influence the surface land temperature. There have been studies comparing temperatures of Kumasi and Accra using Ghana's meteorological stations data [23]. Others, such as [24] have used Landsat data to quantify the extent of green cover loss in Kumasi and its impact on surface temperatures. In Accra, [25] used satellite data to

investigate the relationship between Land Surface Temperature (LST) and vegetation abundance in the Accra Metropolitan Area. It is important to note that none of these studies in Accra and Kumasi was specifically focused on comparing Land Surface Temperature (LST) of the two cities using Landsat 8 satellite data. The objective of our study is to retrieve the LST over Accra and compare the trend and average value of LST with Kumasi using Landsat-8 Operational Land Imager (OLI) thermal infrared satellite data. These two cities were chosen because of the location. While Accra serves as capital, it is located on the Gulf of Guinea along the Atlantic Ocean. Kumasi on the other hand, serves as administrative and commercial center, and it is located in the interior of the country in the forest region of Ghana. These two different set of locations will allow this study to investigate the spatial variation of temperatures between the cities.

2. The Study Area

2.1. Accra Metropolitan Area

Accra became the capital city around the year 1877 when the capital city of Gold Coast was moved from Cape coast. Accra is globally known to be the capital of Ghana situated along the Atlantic coast of the Gulf of Guinea (**Figure 1**). It covers an area of about 225.67 km^2 (87.13 sq mi). The region has a tropical savanna climate with rainy and dry seasons. The rainy season spans from April to mid-July and October and temperatures hoover around 24˚C and 28˚C all year round. The rainfall of Accra is usually down below 800 mm (31.5 in) [26]. The months that Accra experiences heavy rainfall are May and June. Occasionally the first half of July experiences also heavy rainfall [26]. Odaw River flows through Accra with approximately 60% of the Metropolis living in its catchment [27]. According to the Ghana Statistical Services [28], Greater Accra region has a

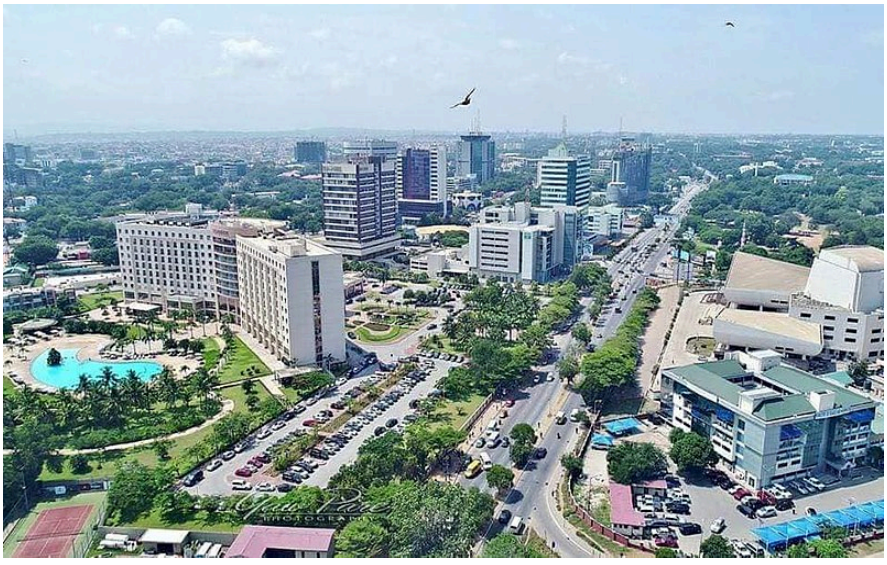

Figure 1. Study area (Accra). Image courtesy [29].

population of about 5,055,883 becoming the most populated city in Ghana [28], [29]. Accra's rapid population growth and physical expansion occurred in an unstable economic environment marked by nearly a decade of economic stagnation in the mid-1970s and early 1980s, followed by nearly two decades of structural change [30]. The region has experienced tremendous growth in population over the years.

Accra is known to be the economic and industrial hub of Ghana. Some economic activities in the region includes, trading, clothing and textiles, the financial and commercial sectors, fishing, and the manufacture of processed foods. Accra is also well noted for its historic travel destinations and is characterized by beautiful beaches along the coast with various resorts. This has become a thriving source of income for people in the tourism industry such as tourist guides, those in the arts and craft industries, travel and tour agents etc. Some major tourist sites in the region includes Jamestown light house, Kwame Nkrumah Memorial Park, Arts Center for National Culture amongst others. Accra has recently become the focus of international research and assistance programs regarding the health and socioeconomic issues of a dense urban population.

2.2. Kumasi Metropolitan Area

Popularly known as Oseikrom, Kumasi boasts of about 36.2 percent of the total population of Ashanti region which estimates to about 1,730,249 people according to the Ghana Statistical Service [20]. It is also known to be the "Garden city" in the past due to the numerous flowering species found in the region. Kumasi covers an estimated area of about 250 square kilometers (km^2). It is located in the transitional forest zone of Ghana and is about 270 km north-west of Accra [31]. The region is characterized by a bi-modal rainfall system; thus, its major raining season begins from April to June and minor seasons in September and October. Kumasi has a tropical climate and is sited in the semi deciduous ecological zone of Ghana. Kumasi is drained by several rivers and streams including the Aboabo and Sisa rivers that flow through the city centers [32]. Trees around River Aboabo have been cut down to provide space for human settlements and hence, increased erosion leading to siltation of the river and flooding [32].

According to [33], about 55% of Kumasi Metropolitan Area is occupied by Urban green space of which about 61% is composed of tree cover such as home gardens, plantations, natural forest, parks, grasslands and farmlands. Kumasi is the home of Ghana's gold and cocoa and is the central point for most commercial activities due to its geographical position (**Figure 2**).

Following Ghana's independence from the British in 1957, Kumasi was designated as the capital of the Ashanti region. The city is still an important trading center and is involved in a variety of industries, including the manufacturing of agricultural products and timber, as well as the manufacture of consumer goods such as textiles and foodstuffs. Kumasi is home to a number of educational institutions, including Komfo Anokye Teaching Hospital, Kwame Nkrumah

Figure 2. Study area (Kumasi and its environs) [34].

University of Science and Technology and Wesley College. Kumasi's physical structure is concentric, with undulating landforms forming slopes and ridges. The metropolis's spatial structure has promoted growth in all direction [35].

2.3. Data Collection

Landsat 8 (Operational Land Imager) images listed in covering Accra, Ghana were acquired from the United States Geological Survey Earth Explorer free Online Data Services for land Surface Temperature (LST) analysis [36]. The images were acquired with minimum cloud cover (<10%) from both dry and rainy seasons (**Table 1**). Accra's dry season is between December to March and the rainy season between May to August. The footprints of the images are shown in **Figures 3-6**.

2.4. Image Processing

To process the images, three tasks were performed. These included: Image preprocessing and rectification.

2.4.1. Image Pre-Processing

In Image pre-processing, both visual and digital image processing were done, and prior to image processing, images were imported into ArcGIS 10.8 Software for further processing. Thermal Infrared bands *i.e.* bands 10 and 11 were selected for further analysis. Accra and Kumasi shapefiles were used to extract from the full scenes to subset the area of interest.

2.4.2. Image Rectifications

Image rectifications were performed in order to correct the data for distortion which may have been developed from the image acquisition process using the Impact toolbox developed by the European Union Joint Research Centre. To ensure accurate identification of temporal changes and geometric compatibility with other sources of information, the images were geocoded to the coordinate

Table 1. Landsat images used in the land surface temperature mapping of Accra.

Reference year	Sensor	Resolution	WRS: P/R	Date of Acquisition	Season	Study area
2020	Landsat 8	30 m	193/056	2020/01/20	Dry	Accra
2020	Landsat 8	30 m	193/056	2020/08/13	Rainy	
2020	Landsat 8	30 m	194/055	2020/01/25	Dry	Kumasi
2020	Landsat 8	30 m	194/055	2020/05/16	Rainy	

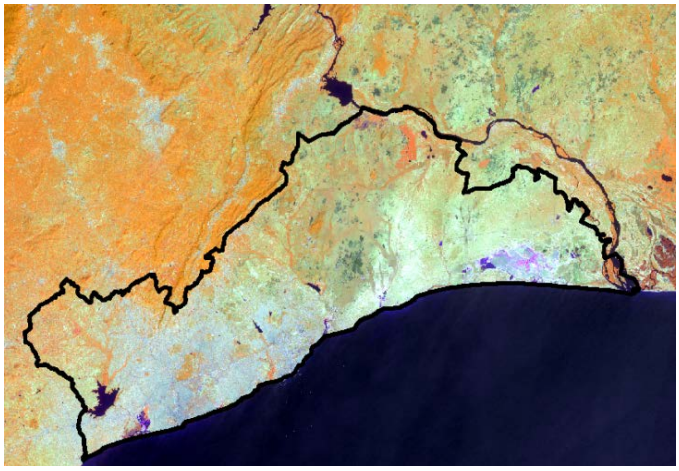

Figure 3. Footprint of Landsat imagery in the study area shown in false color composite from dry season.

Figure 4. Footprint of Landsat imagery in the study area shown in false color composite from rainy season.

and mapping system of the national topographic maps. All the images were projected to the Universal Traverse Mercator (UTM) coordinates zone 30 North. The spheroid and datum was also referenced to WSG84.

2.5. Image Analysis

The algorithm was created in ArcGIS 10.8. In this study Landsat 8 Thermal

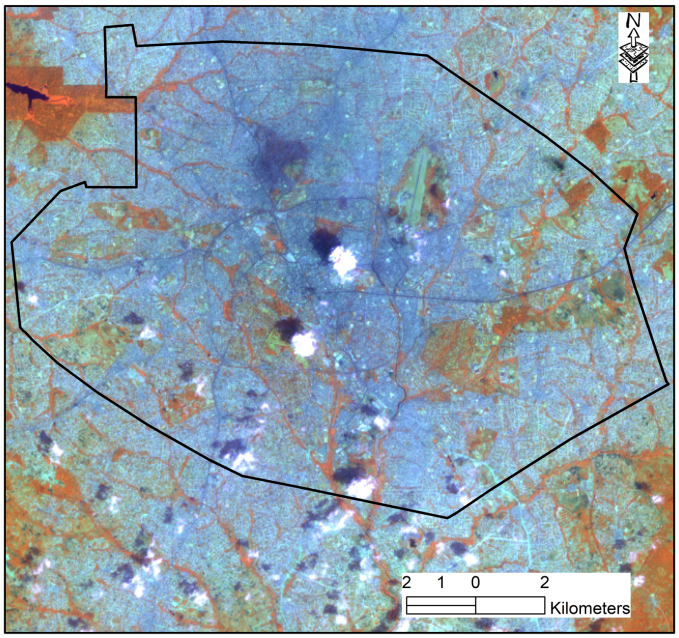

Figure 5. Footprint of Landsat imagery in the study area shown in false color composite dry season 2020.

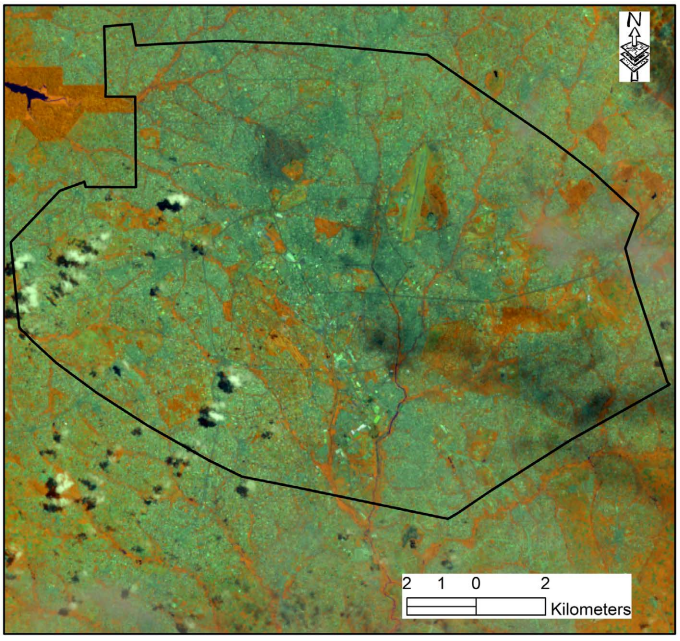

Figure 6. Footprint of Landsat imagery in the study area shown in false color composite from rainy 2020.

Infrared bands (Band 10 and band 11) were used to estimate brightness temperatures and bands 4 and 5 were used for calculating the NDVI. The LST retrieval formulas were taken from the USGS web page for retrieving the top of atmospheric (TOA) spectral radiance [37]. The LST was retrieved following the steps of **Figure 7**. The metadata of the satellite images used in the algorithm is presented in **Table 2**.

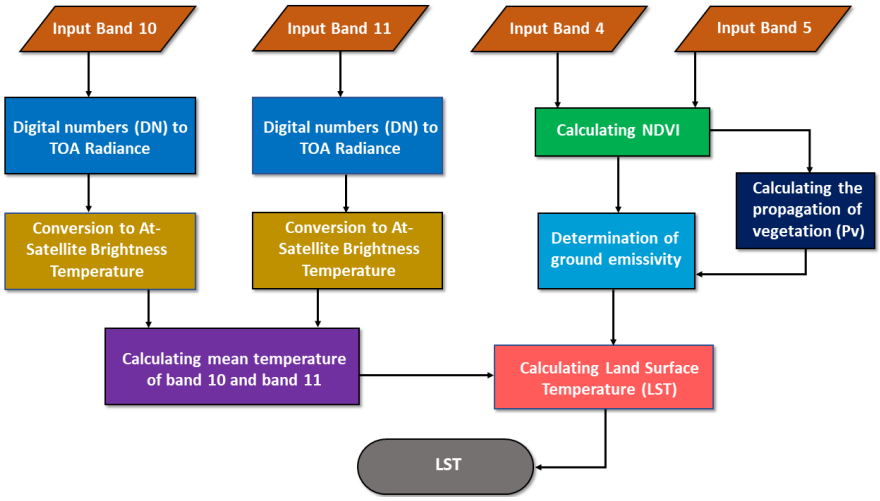

Figure 7. Flowchart for LST retrieval [38].

Table 2. Metadata of the satellite images.

Date	Sensor ID	Resolution	Scene Center Time	Cloud (%)	Location
02 January 2020	OLI and TIRS	30 m	10:15:54.6031820Z	0.01	Accra
13 August 2020	OLI and TIRS	30 m	10:15:41.4738290Z	2.48	
25 January 2020	OLI and TIRS	30 m	10:15:54.6031820Z	0.01	Kumasi
16 May 2020	OLI and TIRS	30 m	10:20:54.1458440Z	30.04	

2.5.1. Converting Digital Numbers (DN) to Top of Atmospheric Spectral Radiance (TOA)

The Thermal band data DN was converted to TOA spectral radiance using the radiance rescaling factors provided in the metadata file [38].

$$L_\lambda = M_L Q_{cal} + A_L \tag{1}$$

where

L_λ = TOA spectral radiance (Watts/(m²*srad*μm));

M_L = Band-specific multiplicative rescaling factor from the metadata (RADIANCE_MULT_BAND_x, where x is the band number);

A_L = Band-specific additive rescaling factor from the metadata (RADIANCE_ADD_BAND_x, where x is the band number);

Q_{cal} = Quantized and calibrated standard product pixel values (DN).

2.5.2. Conversion of TOA to At-Satellite Brightness Temperature

Thermal band data can be converted from spectral radiance to top of atmosphere brightness temperature using the thermal constants in the MTL file [38]:

$$BT = \frac{K_2}{\ln\left[\left(\frac{K_1}{L_\lambda}\right)+1\right]} - 273.15 \tag{2}$$

where

BT = *Top of atmosphere brightness temperature* (K);

L_λ = TOA spectral radiance (Watts/(m²*srad*μm));

K_1 = Band-specific thermal conversion constant from the metadata (K_1_CONSTANT_BAND_x, where x is the thermal band number);

K_2 = Band-specific thermal conversion constant from the metadata (K_2_CONSTANT_BAND_x, where x is the thermal band number).

2.5.3. Calculating NDVI

The normalized difference vegetation index (NDVI), which is derived from remote-sensing (satellite) data, is closely linked to drought conditions. To determine the density of green on a patch of land, the distinct colors (wavelengths) of visible and near-infrared sunlight reflected by the plants are observed; red and near-infrared bands *i.e.* Band 4 and Band 5 respectively were used for calculating the Normal NDVI. The importance of estimating the NDVI is essential since the amount of vegetation present is an important factor and NDVI can be used to infer general vegetation condition. The calculation of the NDVI is important because, afterward, the proportion of the vegetation (P_V) should be calculated, and they are highly related with the NDVI, and emissivity (ε) should be calculated, which is related to the P_V [34].

$$\mathrm{NDVI} = \frac{NIR(\text{band } 5) - R(\text{band } 4)}{nir(\text{band } 5) + r(\text{band } 4)} \tag{3}$$

where NIR represents the near-infrared band (Band 5) and R represents the red band (Band 4).

2.5.4. Calculating the Proportion of Vegetation

Proportion of vegetation (Vegetation Fraction) is defined as the percentage of vegetation occupying the ground area in vertical projection. Changes in vegetation cover directly impact surface water and energy budgets through plant transpiration, surface albedo, emissivity, and roughness [39]. The proportion of vegetation P_v is closely related to NDVI values for vegetation and soil. In this study, P_V was estimated following the NDVI traditional method [40].

$$P_v = \left(\frac{\mathrm{NDVI} - \mathrm{NDVI}_s}{\mathrm{NDVI}_v - \mathrm{NDVI}_s} \right)^2 \tag{4}$$

where NDVI_v and NDVI_s are Maximu and Minmum NDVI respectively representing NDVI of Vegetation and NDVI of soil respectively.

2.5.5. Calculating Land Surface Emissivity

Land surface emissivity (LSE). Average emissivity of an element of the surface of the Earth calculated from measured radiance and land surface temperature. The land surface emissivity (LSE (ε)) must be known in order to estimate LST, ince the LSE is a proportionality factor that scales blackbody radiance (Planck's law) to predict emitted radiance, and it is the efficiency of transmitting thermal ener-

gy across the surface into the atmosphere [41]. The determination of the ground emissivity is calculated conditionally as suggested [42].

$$\varepsilon_{\lambda} = \varepsilon_{v\lambda} P_v + \varepsilon_{s\lambda}\left(1 - P_v\right) + C_{\lambda}, \tag{5}$$

where ε_v and ε_s are the vegetation and soil emissivities, respectively, and C represents the surface roughness ($C = 0$ for homogenous and flat surfaces) taken as a constant value of 0.005 [43]. The condition can be represented with the following formula and the emissivity constant values shown [38].

$$\varepsilon_{\lambda} = \begin{cases} \varepsilon_{s\lambda}, & \mathrm{NDVI} < \mathrm{NDVI}_s, \\ \varepsilon_{v\lambda} P_v + \varepsilon_{s\lambda}\left(1 - P_v\right) + C, & \mathrm{NDVI}_s \le \mathrm{NDVI} \le \mathrm{NDVI}_v \\ \varepsilon_{s\lambda} + C, & \mathrm{NDVI} < \mathrm{NDVI}_v, \end{cases} \tag{6}$$

When the NDVI is less than 0, it is classified as water, and the emissivity value of 0.991 is assigned. For NDVI values between 0 and 0.2, it is considered that the land is covered with soil, and the emissivity value of 0.996 is assigned. Values between 0.2 and 0.5 are considered mixtures of soil and vegetation cover and [44] is applied to retrieve the emissivity. In the last case, when the NDVI value is greater than 0.5, it is considered to be covered with vegetation, and the value of 0.973 is assigned. However for this study the mean NDVI value is between 0 and 0.2 therefore the emissivity value of 0.996 was assigned.

2.5.6. Calculating Land Surface Temperature

LST or the emissivity corrected land surface temperature T_s is computed as follows [45]:

$$T_s = \frac{BT}{1 + \left[\left(\frac{\lambda BT}{\rho}\right)\ln \varepsilon_{\lambda}\right]} \tag{7}$$

where T_s is the LST in Celsius (˚C, (2)), BT is at-sensor BT(˚C), λ is the wavelength of emitted radiance (for which the peak response and the average of the limiting wavelength (λ = 10.895) [46] will be used), ε_{λ} is the emissivity calculated in [44] [47] and [48].

$$\rho = h\frac{c}{\sigma} = 1.438 \times 10^{-2}\ \mathrm{m \cdot K} \tag{8}$$

where σ is the Boltzmann constant (1.38×10^{-23} J/K), h is Planck's constant (6.626×10^{-34} J s), and c is the velocity of light (2.998×10^{8} m/s) [46] [47].

3. Results, Discussion and Conclusion

Results of Accra LST from the dry and rainy seasons are shown in **Figure 8** and **Figure 9**. **Figure 10** shows Kumasi LST from January 2020 (dry season). **Figure 11** displays Kumasi LST from May 2020. In Accra, the temperatures ranges during the dry seasons were found in this study to range from 21.0985˚C to 46.1314˚C. In the wet seasons the recorded temperatures were lower than those recorded in the dry seasons and ranged from 18.3437˚C to 30.9693˚C. Results of

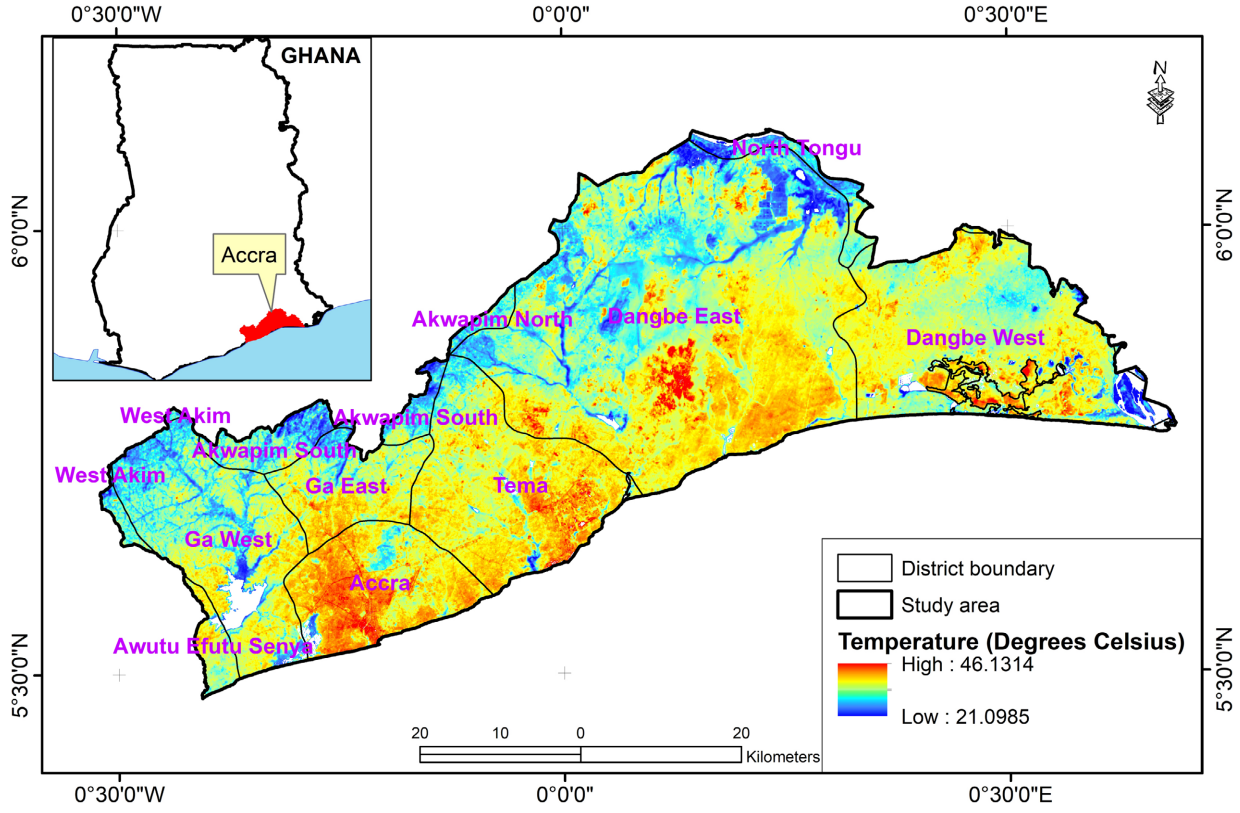

Figure 8. Accra LST from dry season.

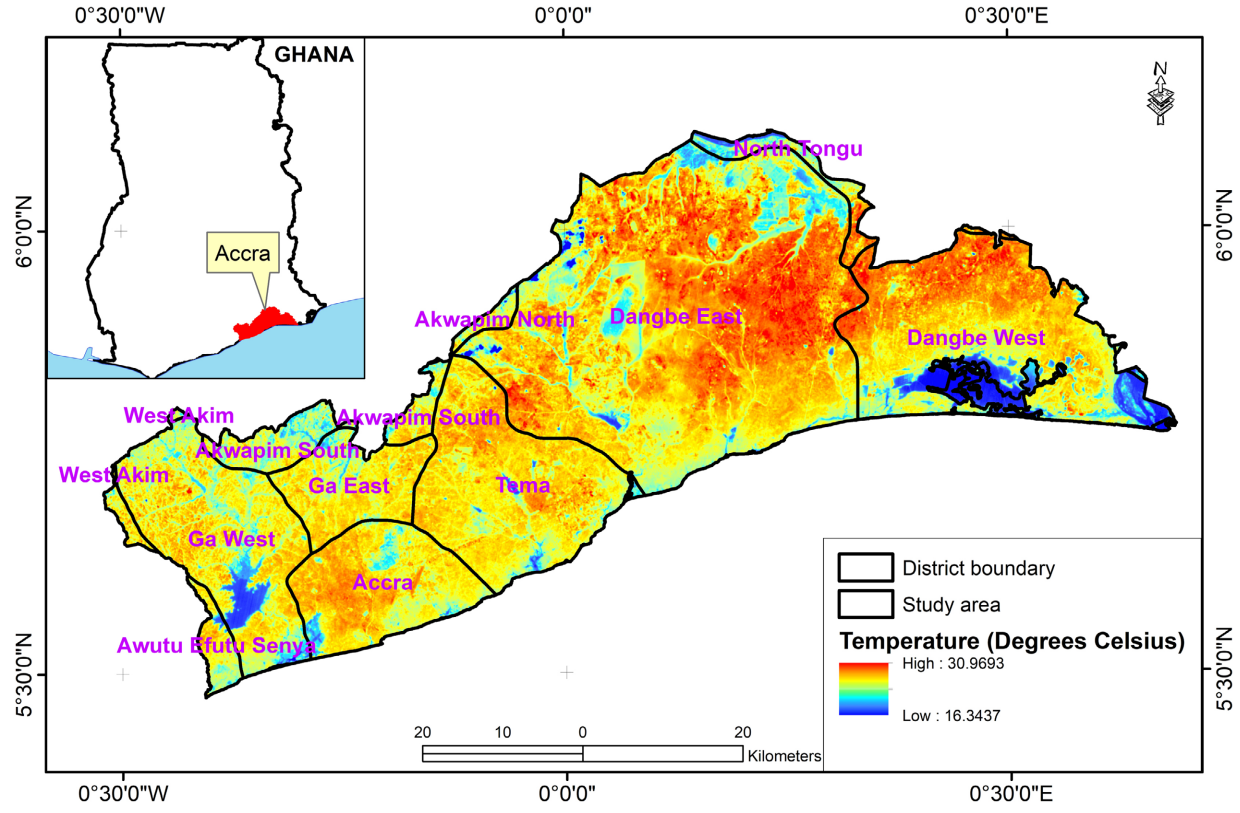

Figure 9. Accra LST from rainy season (August).

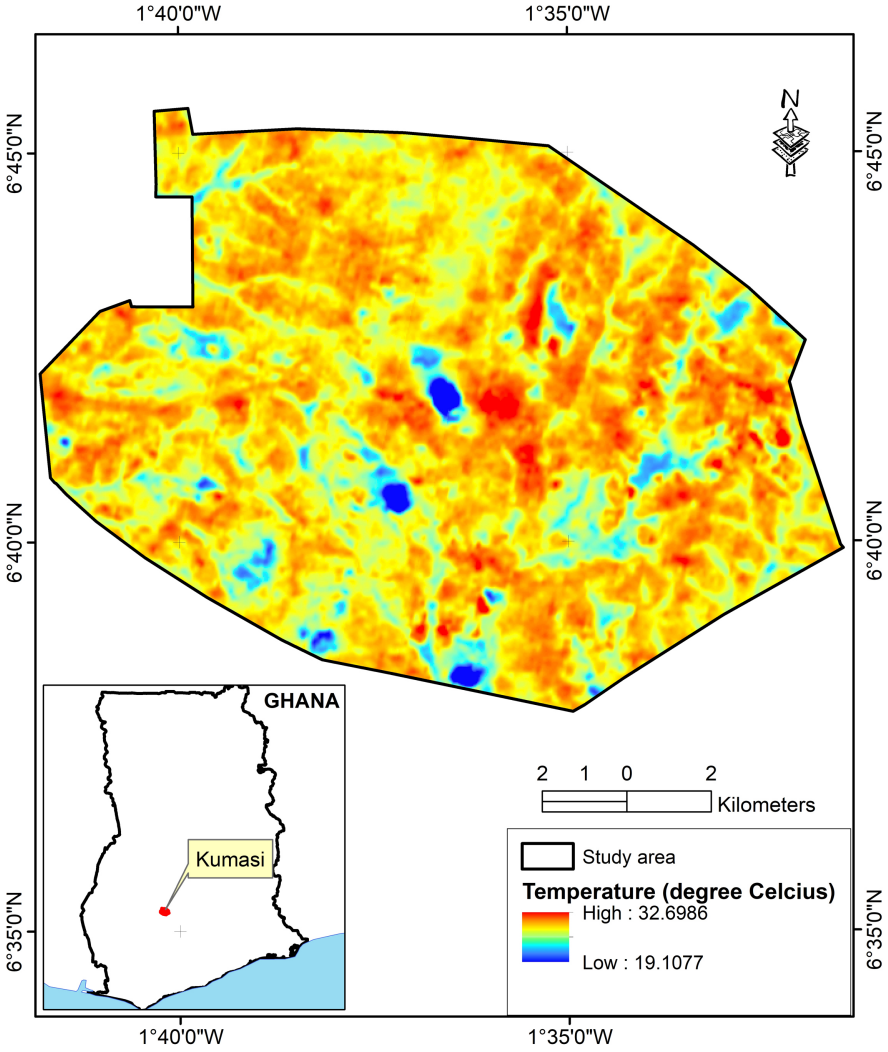

Figure 10. Kumasi LST from January 2020 (dry season).

Kumasi also shows a higher range of temperatures from 32.6986˚C to 19.1077˚C during the dry season. In the wet season, temperatures ranged from 26.4142˚C to −0.898728˚C. Accra and Kumasi have undergone growth in terms of populations and economy. In an attempt to cater for the demand for housing for the population and strictures for formal and informal industries, expansion in land covered by impermeable cover has taken place. Meanwhile, the natural land surfaces (green vegetation, soil and water) are interfered with.

4. Discussion

Urbanization has greatly affected developing countries throughout the world differently at rates varying from moderate to rapid. For most cities in these countries, the initial cause of population growth is attributed to rural-urban migration, while latter growth is mainly linked to babies born to city immigrants [49]. Like many cities in developing countries, Accra and Kumasi have been undergoing population and economic growths respectively. Meanwhile, impervious

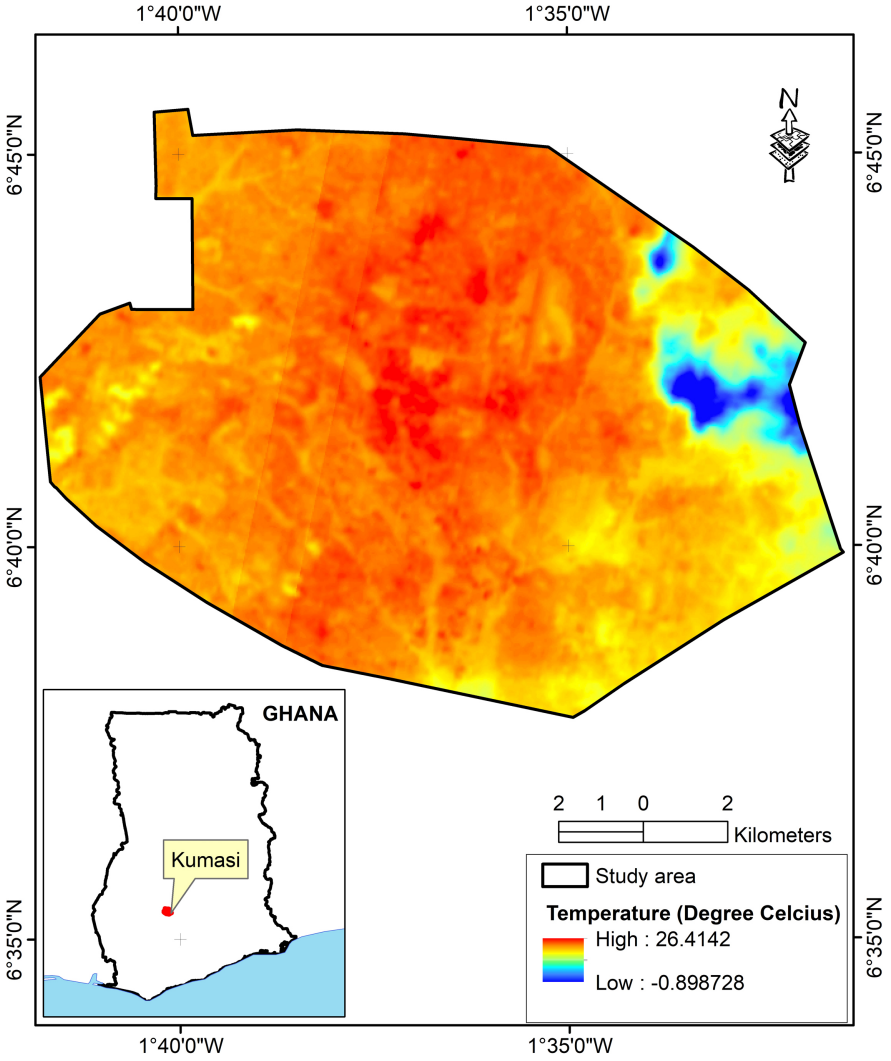

Figure 11. Kumasi LST from May 2020.

surfaces and structures have been constructed on land that was once covered with urban greenery, resulting in the cities experiencing warmer temperatures than rural areas through the urban heat island's phenomenon.

Research shows that land surface temperature is positively correlated with the proportion of land covered by built up (low density and high density) and negatively correlated with the percentage of forest, farmland, and water bodies per grid cell. The replacement of vegetation by asphalt and concrete for construction of roads, buildings, and other structures for accommodation of growing urban populations and industries, etc., leads to the formation of urban heat islands [5]. Anthropogenic heat emission generated by human population distribution also influences the intensity of urban heat islands [6], a significant contributor to the urban's land surface temperatures. Other factors that that influence land surface temperature are, the color of buildings, traffic loads, the sky view factor, the physical properties of structures, street geometry, view factor of the sky and human activities [4].

Heat islands form as vegetation is replaced by asphalt and concrete for roads, buildings, and other structures necessary to accommodate growing urban populations. Instead of reflecting away the thermal energy transmitted to them from the sun, such surfaces absorb it, leading to rising of surface temperatures and overall ambient temperatures. Removal of trees and vegetation lowers the natural cooling effects of shading and evaporation of water from soil and leaves (evapotranspiration).

Also, the geometry and dimensions of the urban structures dictate the air flow in the streets and hence, interfere with natural thermal and fluid flow through the streets respectively [50]. Both of the discussed scenarios exist in Accra and Kumasi, making them experience elevated temperatures with respect to corresponding rural areas. During some days of the dry seasons, the results show that temperatures exceeding human body average temperature were recorded in Accra. With the growth of population, decrease in urban greenery, construction of more impervious structures and air pollution, the temperatures may gradually rise to critical levels that are risky to human life.

5. Conclusion

The high temperatures computed during part of the year for these cities, especially Accra can impact human health and comfort. While global warming is a universal phenomenon, urban greenery should be increased to mitigate for contribution to the metropolitans' contribution to the temperature in terms of urban heat islands' effect. Trees also remove significant quantities of air pollutants and hence, could boost the quality of lives in Accra and Kumasi. The findings of this study can be used to inform and guide urban land planners and leaders to appreciate the importance of urban green spaces. The study can be informative to Accra and Kumasi stakeholders on the influence of land use/land cover on urban land surface temperature. The results of this study can bring to the attention of local leaders the urgency of proposing policies that will be adopted for future plans to expand the cities to accommodate the growing populations while and mitigate rising urban temperatures, respectively. Finally, the land surface temperature (LST) results in this study could be used to better understand spatial variation in temperature of the two cities. This will allow city planners to sustainably plan the two cities by reducing Urban Heat Island effect.

Acknowledgements

This work was supported by the United States Department of Agriculture (USDA) National Institute of Food and Agriculture, McIntire Stennis Project NI21MSCFRXXXG003. Also, we would like to extend our sincere gratitude to the Dean of Graduate Studies at Southern University in Baton Rouge, Louisiana, Professor Ashagre Yigletu for providing graduate assistantships to some of the graduate students on this paper in order to promote research and help the students acquire the necessary skill development while earning a graduate degree.

Conflicts of Interest

The authors declare no conflicts of interest regarding the publication of this paper.

References

[1] Voogt, J.A. and Oke, T.R. (2003) Thermal Remote Sensing of Urban Climates. *Remote Sensing of Environment*, **86**, 370-384. https://doi.org/10.1016/S0034-4257(03)00079-8

[2] Xiao, R., Weng, Q., Ouyang, Z., Li, W., Schienke, E.W. and Zhang, Z. (2008) Land Surface Temperature Variation and Major Factors in Beijing, China. *Photogrammetric Engineering & Remote Sensing*, **74**, 451-461. https://doi.org/10.14358/PERS.74.4.451

[3] Voogt, J.A. and Oke, T.R. (1998) Effects of Urban Surface Geometry on Remotely-Sensed Surface Temperature. *International Journal of Remote Sensing*, **19**, 895-920. https://doi.org/10.1080/014311698215784

[4] Chudnovsky, A., Ben-Dor, E. and Saaroni, H. (2004) Diurnal Thermal Behavior of Selected Urban Objects Using Remote Sensing Measurements. *Energy and Buildings*, **36**, 1063-1074. https://doi.org/10.1016/j.enbuild.2004.01.052

[5] Valsson, S. and Bharat, A. (2009) Urban Heat Island: Cause for Microclimate Variations. *Architecture- Time Space & People*, **2125**.

[6] Fan, H. and Sailor, D.J. (2005) Modeling the Impacts of Anthropogenic Heating on the Urban Climate of Philadelphia: A Comparison of Implementations in Two PBL Schemes. *Atmospheric Environment*, **39**, 73-84. https://doi.org/10.1016/j.atmosenv.2004.09.031

[7] Feng, Y., Gao, C., Tong, X., Chen, S., Lei, Z. and Wang, J. (2019) Spatial Patterns of Land Surface Temperature and Their Influencing Factors: A Case Study in Suzhou, China. *Remote Sensing*, **11**, Article No. 182. https://doi.org/10.3390/rs11020182

[8] Oke, T.R., Spronken-Smith, R.A., Jauregui, E. and Grimmond, C.S.B. (1999) The Energy Balance of Central Mexico City during the Dry Season. *Atmospheric Environment*, **33**, 3919-3930. https://doi.org/10.1016/S1352-2310(99)00134-X

[9] Tong, H., Walton, A., Sang, J. and Chan, J.C.L. (2005) Numerical Simulation of the Urban Boundary Layer over the Complex Terrain of Hong Kong. *Atmospheric Environment*, **39**, 3549-3563. https://doi.org/10.1016/j.atmosenv.2005.02.045

[10] Saitoh, T.S., Shimada, T. and Hoshi, H. (1996) Modeling and simulation of the Tokyo urban heat island. *Atmospheric Environment*, **30**, 3431-3442. https://doi.org/10.1016/1352-2310(95)00489-0

[11] Cendese, A. and Monti, P. (2003) Interaction between an Inland Urban Heat Island and a Sea-Breeze Flow: A Laboratory Study. *Journal of Applied Meteorology and Climatology*, **42**, 1569-1583. https://doi.org/10.1175/1520-0450(2003)042%3C1569:IBAIUH%3E2.0.CO;2

[12] Streutker, D.R. (2003) Satellite-Measured Growth of the Urban Heat Island of Houston, Texas. *Remote Sensing of Environment*, **85**, 282-289. https://doi.org/10.1016/S0034-4257(03)00007-5

[13] McNeill, J., Alves, D., Arizpe, L., Bykova, O., Galvin, K., Kelmelis, J., Migot-Adholla, S., Morrisette, P., Moss, R., Richards, J. and Riebsame, W. (1994) Toward a Typology and Regionalization of Land-Cover and Land-Use Change: Report of Working Group B. In: Meyer, W.B. and Turner II, B.L., Eds., *Changes in Land Use and Land*

Cover: *A Global Perspective*, Vol. 4, Cabridge university press, Cambridge, 55-71.

[14] Laurance, W.F., Albernaz, A.K.M., Schroth, G., Fearnside, P.M., Bergen, S., Venticinque, E.M. and Da Costa, C. (2002) Predictors of Deforestation in the Brazilian Amazon. *Journal of Biogeography*, **29**, 737-748. https://doi.org/10.1046/j.1365-2699.2002.00721.x

[15] Allen, J.C. and Barnes, D.F. (1985) The Causes of Deforestation in Developing Countries. *Annals of American Association of Geographers*, **75**, 163-184. https://doi.org/10.1111/j.1467-8306.1985.tb00079.x

[16] Attua, E.M. and Fisher, J.B. (2011) Historical and Future Land-Cover Change in a Municipality of Ghana. *Earth Interact*, **15**, 1-26. https://doi.org/10.1175/2010EI304.1

[17] Konadu-Agyemang, K. (2001) The Political Economy of Housing and Urban Development in Africa: Ghana's Experience from Colonial Times to 1998. Praeger Publishers, Westport.

[18] Ghana Statistical Service (GSS) (2013) Population and Housing Census 2010. http://www.statsghana.gov.gh/

[19] World Bank (2015) Rising through the Cities in Ghana. Ghana Urbanization Review Overview Report. World Bank Group, Washington DC.

[20] Ghana Statistical Service (2014) 2010 Population and Housing Census. District Analytical Report. Kumasi Metropolitan. Ghana Statistical Service, Accra. https://www2.statsghana.gov.gh/docfiles/2010_District_Report/Ashanti/KMA.pdf

[21] Yilmaz, S., Toy, S., Yildiz, N.D. and Yilmaz, H. (2009) Human Population Growth and Temperature Increase along with the Increase in Urbanisation, Motor Vehicle Numbers and Green Area Amount in the Sample of Erzurum City, Turkey. *Environmental Monitoring and Assessment*, **148**, 205-213. https://doi.org/10.1007/s10661-007-0151-z

[22] Addae, B. and Oppelt, N. (2019) Land-Use/Land-Cover Change Analysis and Urban Growth Modelling in the Greater Accra Metropolitan Area (GAMA), Ghana. *Urban Science*, **3**, Article No. 26. https://doi.org/10.3390/urbansci3010026

[23] Manu, A., Twumasi, Y.A. and Coleman, T.L. (2006) Is It Global Warming or the Effect of Urbanization? The Rise in Air Temperature in Two Cities of Ghana. *Proceedings of the* 5*th International Federation of Surveyors* (*FIG*) *Regional Conference for Africa*, Accra, 8-11 March 2006, 1-14. http://www.fig.net/resources/proceedings/fig_proceedings/accra/papers/ts23/ts23_02_manu_etal.pdf

[24] Mensah, C., Atayi, J., Kabo-Bah, A.T., Švik, M., Acheampong, D., Kyere-Boateng, R., Prempeh, N.A. and Marek, M.V. (2020) Impact of Urban Land Cover Change on the Garden City Status and Land Surface Temperature of Kumasi. *Cogent Environmental Science*, **6**, Article ID: 1787738. https://doi.org/10.1080/23311843.2020.1787738

[25] Mantey, S., Tagoe, N.D. and Abaidoo, C.A. (2014) Estimation of Land Surface Temperature and Vegetation Abundance Relationship—A Case Study. 3*rd UMaT Biennial International Mining and Mineral Conference*, Tarkwa, 30 July-2 August 2014, 1-10.

[26] Musah, A.-A.I., Du, J., Udimal, T.M. and Sadick, M.A. (2018) The Nexus of Weather Extremes to Agriculture Production Indexes and the Future Risk in Ghana. *Climate*, **6**, Article No. 86. https://doi.org/10.3390/cli6040086

[27] Abraham, E.M., Drechsel, P. and Cofie, O. (2006) The Challenge of Urban Flood Control: The Case of Accra's Korle Lagoon. *5th Worldwide Workshop for Young*

Environmental Scientist in France, Vitry sur Seine, 9-12 May 2006. https://publications.iwmi.org/pdf/H038739.pdf

[28] Ghana Statistical Service (2020) Population and Housing Census Report. Regional Office, Accra. https://statsghana.gov.gh

[29] Amanor, K. (2018) A Drone Footage of Accra Central, Ghana. Wikimedia Commons.

[30] Songsore, J. (2008) Environmental and Structural Inequalities in Greater Accra. *Journal of the International Institute*, **16**, 8-13. http://hdl.handle.net/2027/spo.4750978.0016.105

[31] Simon, D., McGregor, D. and Nsiah-Gyabaah, K. (2004) The Changing Urban-Rural Interface of African Cities: Definitional Issues and an Application to Kumasi, Ghana. *Environment and Urbanization*, **16**, 235-248. https://doi.org/10.1177%2F095624780401600214

[32] Oppong, B. (2011) Environmental Hazards in Ghanaian Cities: The Incidence of Annual Floods along the Aboabo River in the Kumasi Metropolitan Area (KMA) of the Ashanti Region of Ghana. Doctoral Dissertation, Department of Geography and Rural Development, Kwame Nkrumah University of Science and Technology, Ghana. http://ir.knust.edu.gh/xmlui/handle/123456789/2080

[33] Nero, B.F., Callo-Concha, D., Anning, A. and Denich, M. (2017) Urban Green Spaces Enhance Climate Change Mitigation in Cities of the Global South: The Case of Kumasi, Ghana. *Procedia Engineering*, **198**, 69-83. https://doi.org/10.1016/j.proeng.2017.07.074

[34] Serwaa, J. (2021, March 4) 4K Drone View of the Real Kumasi Garden City: Beautiful and Well Planned Areas to Live in Kumasi. https://www.youtube.com/watch?v=R_mHrfLt568

[35] Kumasi Metropolitan Assembly (2005) Medium Term Development Plan, 2005-2009. An Unpublished Document Prepared to Guide the Development of the Kumasi Metropolis in the Medium Term.

[36] U.S. Geological Survey (2019) EarthExplorer-Home. Satellite Data. https://earthexplorer.usgs.gov/

[37] U.S. Geological Survey (2021) Landsat Missions: Using the USGS Landsat Level-1 Data Product. https://www.usgs.gov/core-science-systems/nli/landsat/using-usgs-landsat-level-1-data-product

[38] Avdan, U. and Jovanovska, J. (2016) Algorithm for Automated Mapping of Land Surface Temperature Using LANDSAT 8 Satellite Data. *Journal of Sensors*, **2016**, Article ID: 1480307. https://doi.org/10.1155/2016/1480307

[39] Aman, A., Randriamanantena, H.P., Podaire, A. and Froutin, R. (1992) Upscale Integration of Normalized Difference Vegetation Index: The Problem of Spatial Heterogeneity. *IEEE Transactions on Geoscience and Remote Sensing*, **30**, 326-338. https://doi.org/10.1109/36.134082

[40] Rouse, J.W., Haas, R.W., Schell, J.A., Deering, D.W. and Harlan, J.C. (1974) Monitoring the Vernal Advancements (Greenwave Effect) and Retrogradation of Natural Vegetation. NASA/GSFCT Type III Final Report, Texas A & M University, Remote Sensing Center, College Station, 1-137.

[41] Jimenez-Munoz, J.C., Sobrino, J.A., Gillespie, A., Sabol, D. and Gustafson, W.T. (2006) Improved Land Surface Emissivities over Agricultural Areas Using ASTER NDVI. *Remote Sensing of Environment*, **103**, 474-487. https://doi.org/10.1016/j.rse.2006.04.012

[42] Sobrino, J.A., Jiménez-Muñoz, J.C. and Paolini, L. (2004) Land Surface Temperature Retrieval from LANDSAT TM5. *Remote Sensing of Environment*, **90**, 434-440. https://doi.org/10.1016/j.rse.2004.02.003

[43] Sobrino, J.A. and Raissouni, N. (2000) Toward Remote Sensing Methods for Land Cover Dynamic Monitoring: Application to Morocco. *International Journal of Remote Sensing*, **21**, 353-366. https://doi.org/10.1080/014311600210876

[44] Barsi, J.A., Schott, J.R., Hook, S.J., Raqueno, N.G., Markham, B.L. and Radocinski, R.G. (2014) Landsat-8 Thermal Infrared Sensor (TIRS) Vicarious Radiometric Calibration. *Remote Sensing*, **6**, 11607-11626. https://doi.org/10.3390/rs61111607

[45] Stathopoulou, M. and Cartalis, C. (2007) Daytime Urban Heat Islands from Landsat ETM+ and Corine Land Cover Data: An Application to Major Cities in Greece. *Solar Energy*, **81**, 358-368. https://doi.org/10.1016/j.solener.2006.06.014

[46] Barsi, J.A., Lee, K., Kvaran, G., Markham, B.L. and Pedelty, J.A. (2014) The Spectral Response of the Landsat-8 Operational Land Imager. *Remote Sensing*, **6**, 10232-10251. https://doi.org/10.3390/rs61010232

[47] Azua, S., Nnah, S.I. and Ikwueze, H.U. (2020) Spatio-Temporal Variability of Landuse Landcover and Its Impact on Land Surface Temperature in Zaria Metropolis, Nigeria. *FUTY Journal of the Environment*, **14**, 1-11.

[48] Xu, H.Q. and Chen, B.Q. (2004) Remote Sensing of the Urban Heat Island and Its Changes in Xiamen City of SE China. *Journal of Environmental Sciences*, **16**, 276-281.

[49] Gilbert, A. (1992) Third World Cities: Housing, Infrastructure and Servicing. *Urban Studies*, **29**, 435-460. https://doi.org/10.1080%2F00420989220080521

[50] Akubue, J.A. (2019) Effects of Street Geometry on Airflow Regimes for Natural Ventilation in Three Different Street Configurations in Enugu City. In: Cakmakli, A.B., Ed., *Different Strategies of Housing Design*, IntechOpen, London.